Journal of Mines, Metals and Fuels, *73(3): 725-741; 2025. DOI: 10.18311/jmmf/2025/48172*

Print ISSN : 0022-2755

Journal of Mines, Metals and Fuels

Contents available at: *www.informaticsjournals.co.in/index.php/jmmf*

Heat and Mass Transfer Through Cuo-Water Maxwell Nano-Fluid in a Horizontal Channel Heated at Center with Slip Effects

P. Rahira[1]*, G. Srinivas[1], P. Suresh[2], G. Murali[1], B. Suresh Babu[3] and T. Haripriya[3]

[1]Geethanjali College of Engineering and Technology, Cheeryal - 501301, Telangana, India; rahi.maths@gmail.com

[2]Chaitanya Bharathi Institute of Technology, Gandipet - 500075, Telangana, India

[3]Sreyas Institute of Engineering and Technology, Hyderabad - 500068, Telangana, India

Abstract

Objectives: *To study the slip effects on heat and mass transfer in a horizontal channel.* ***Methods:*** *The CuO-water Maxwell nanofluid is considered as medium and the heating is through the centre with a heated cylinder throughout the channel. The governing equations lead to system of two dimensional coupled nonlinear partial differential equations. The numerical solution of finite element method is obtained using Mathematica 10.1*

Major Findings: *The study finds that adding CuO nanoparticles (1-5 % composition) increases heat transfer by up to 20 %. An increase in thermal slip from 0.1 to 0.3 reduces the heat transfer rate by 90 %, showing thermal slip's utility in fine-tuning heating or cooling systems. An internal heat source enhances heat transfer in the nanofluid by 32 %, while diffusion slip raises mass transfer by 64 %. These slip effects are therefore crucial in controlling flow dynamics to achieve desired heat and mass transfer rates in industrial applications.* ***Novelty:*** *The study of heat and mass transfer through maxwell nanofluid with the effect of heating at the centre through a cylindrical geometry with slip effects.*

Keywords: *Cuo-Water Maxwell Nanofluid, Finite Element Method, Heat and Mass Transfer, Horizontal Channel, Slip Effects*

1.0 Introduction

Decades of research underscore the critical role of heat and mass transfer studies in diverse industrial applications. Experimental and computational investigations are increasingly vital in addressing the cooling and heating requirements of numerous industrial systems. Building upon the foundational work of Nasir *et al.*[1] subsequent research has significantly advanced the understanding of heat transfer flux in hybrid nanofluids, exploring a wide array of parameters influencing hybrid nanofluid concentrations. Rashid *et al.*[2] highlighted the interfacial region as the locus of maximum heat transfer. Vanaja *et al.*[3] investigated heat and mass transport in micropolar and viscous fluids within vertical tubes, focusing on velocity profiles, slip conditions, and variable viscosity effects. Vasavi *et al.*[4] extended this research to analyze thermal slip effects in vertical channels. Oudina *et al.*[5] conducted a numerical study of mixed convection in a horizontal channel with an open trapezoidal enclosure, demonstrating the significant impact of heat source placement on isotherm distribution through experiments with strategically positioned heat sources. Everts *et al.*[6] employed both computational simulations and experimental validation to analyze the thermal-fluid dynamics of developing mixed convective laminar flow

**Author for correspondence*

in a long horizontal tube (11.52 mm internal diameter, 9.5 m length) under various constant heat flux conditions, concentrating on fully developed laminar duct flow. Ali *et al.*[7] investigated mixed convective flow within a horizontal channel incorporating alternating baffles and an external magnetic field. Mashkour[8] explored transient mixed convection in a partially heated horizontal channel, revealing a positive correlation between the average Nusselt number and the Reynolds number. Alguboori *et al.*[9] examined natural convection heat transfer in horizontal elliptic and inclined enclosures containing a circular internal heat source.

Mat Noor *et al.*[10] investigated the influence of slip on magnetohydrodynamic flow of a Jeffrey nanofluid in a horizontal channel, demonstrating that thermophoresis and viscous dissipation accelerate both the temperature profile and heat transfer rate. Zohra *et al.*[11] modeled nanobio transport in a stretched horizontal channel filled with a micropolar fluid containing gyrotactic microorganisms, analyzing magnetohydrodynamic convective flow, heat and mass diffusion, and Navier slip boundary conditions. Gorbachev and Terekhov[12] numerically studied heat and mass transfer during the evaporative cooling of a moist air stream in a horizontal channel, incorporating the final water layer thickness into their analysis. Nazeer *et al.*[13] explored the impact of electro-osmosis on entropy generation and heat transfer in a horizontal channel containing blood and gold nanoparticles, revealing the influence of slip, Casson fluid behavior, and heat generation on Bejan numbers and entropy. Felicita *et al.*[14] demonstrated that magnetic and buoyancy ratio parameters decelerate flow, while the Weissenberg number exhibits a dual effect on Williamson nanomaterial flow in a microchannel with slip and convective boundary conditions. Babu *et al.*[15] investigated three-dimensional entropy generation in non-linearly stretching sheet nanofluid convective flow, including slip effects, using tabular data to quantify heat transfer rates and surface drag forces. Mahmood *et al.*[16] analyzed the influence of heat generation/absorption and mass suction on stagnation point flow under magnetohydrodynamic conditions over a non-linearly stretching/shrinking tri-hybrid nanofluid sheet.

Boujelbene, Mohamed *et al.*[17] studied the flow of a Prandtl nanofluid over a heated, extending cylindrical surface with interfacial slip. Adnan[18] investigated the Nusselt number in a two-viscosity fluid under discrete heating, finding that convective dominance maximizes heat transfer and that increasing the bi-viscosity parameter magnitude induces secondary circulation (for Pr = 10), directly affecting the heat transfer rate. Optimizing the heat generation parameter relative to the Grashof number yields maximum average and local Nusselt numbers. Cheruku *et al.*[19] explored multiple slip effects. Srikanth *et al.*[20] and Sailaja *et al.*[21] independently analyzed two-dimensional nanofluid heat transfer past a moving vertical plate. Lone *et al.*[22] examined a hybrid nanofluid (copper, alumina, and titanium nanoparticles) over a curved sheet, considering the effects of chemical reactivity, magnetic field, and Joule heating. Gosty Vanaja *et al.*[23] investigated flow, heat, and mass transfer in a vertical channel containing two immiscible fluids, focusing on slip effects. Khan *et al.*[24] analyzed the impact of a temperature-dependent, exponentially varying heat source and non-linear thermal radiation. Further research by Khan *et al.*[25] highlighted the synergistic effects of multiple slip and thermal radiation on heat and mass transfer in hybrid nanofluids under Magneto-Hydro-Dynamic (MHD) conditions. Kumar and Yadav[26] demonstrated the importance of asymmetric porous channels in enhancing flow conditions in complex two-fluid systems, focusing on tilted magnetic fields and slip effects in peristaltic flows of immiscible fluids.Articles[27-59] provide some instances of potential uses.

Examining the flow of heat and mass through a CuO-water Maxwell nanofluid with a cylinder-shaped heat source in the center is the primary objective of this work. This kind of situation arises in many biological and refrigerating systems. Interestingly, the existing literature does not examine the slip effect when a cylindrical shape introduces additional heat. Therefore, our paper seeks to explore the consequences of additional heating from a heated pipe positioned at the channel's center, taking into account velocity, thermal, and diffusion slip effects. capture the intricate relationships between heat and mass transit events by precisely simulating the coupled nonlinear governing equations using the finite element approach.

The visualizations, such as stream plots and contour plots, effectively convey our findings, which are vital for filling the existing gap and offering insights into spatial parameter distributions, thus enhancing understanding of the system's heat and mass transfer characteristics.

2.0 Methodology

The laminar, fully developed, incompressible CuO – water Maxwell nano-fluid is considered in square channel and following assumptions are made to generate the governing equations:

The flow is directed along thez-axis

- A heated hollow cylinder is centrally located, serving as an additional heat source, alongside heating applied to the channel's bottom wall.
- Both top and bottom walls of the channel are thermally conductive.
- The application of the magnetic field is in the y-direction.
- The slip conditions are applied on the heated cylinder's surface.
- On the upper wall: U=0, v=0, T = T_0, C=C_0
- On the lower wall: U=0, v=0, T = T_1, C=C_1

Continuity Equation:

$$\frac{\partial u}{\partial x}+\frac{\partial v}{\partial y}=0 \tag{1}$$

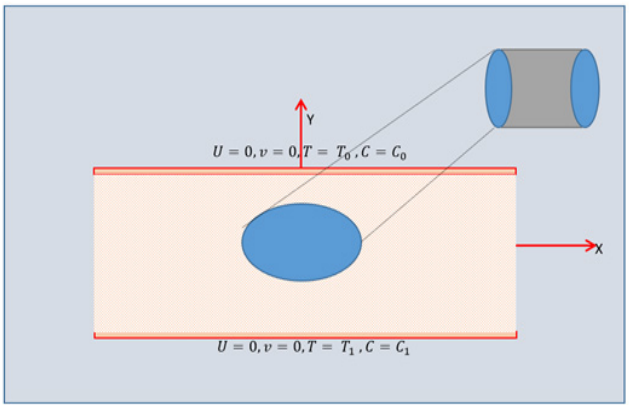


Figure 1. Schematic diagram representing the cross section of the channel.

Momentum Equation:

$$u\left(\frac{\partial u}{\partial x}\right)+v\left(\frac{\partial u}{\partial y}\right)=\nu_{nf}\left(\frac{\partial^2 u}{\partial x^2}+\frac{\partial^2 u}{\partial y^2}\right)-k_o\left(u^2\frac{\partial^2 u}{\partial x^2}+v^2\frac{\partial^2 u}{\partial y^2}+2uv\frac{\partial^2 u}{\partial x\,\partial y}\right) \tag{2}$$

$$u\left(\frac{\partial v}{\partial x}\right)+v\left(\frac{\partial v}{\partial y}\right)=\nu_{nf}\left(\frac{\partial^2 v}{\partial x^2}+\frac{\partial^2 v}{\partial y^2}\right)-\left(\frac{\sigma B_o^2}{\rho_{nf}}\right)v-k_o\left(u^2\frac{\partial^2 v}{\partial x^2}+v^2\frac{\partial^2 v}{\partial y^2}+2uv\frac{\partial^2 v}{\partial x\,\partial y}\right)+g\beta_T(T-T_0)+g\beta_C(C-C_0) \tag{3}$$

Equation of thermal energy:

$$u\left(\frac{\partial T}{\partial x}\right)+v\left(\frac{\partial T}{\partial y}\right)=\alpha_{nf}\left(\frac{\partial^2 T}{\partial x^2}+\frac{\partial^2 T}{\partial y^2}\right)+\tau\left\{D_B\left(\frac{\partial C}{\partial x}\right)\left(\frac{\partial T}{\partial x}\right)+D_B\left(\frac{\partial C}{\partial y}\right)\left(\frac{\partial T}{\partial y}\right)+\frac{D_T}{T_0}\left(\frac{\partial T}{\partial x}\right)^2+\frac{D_T}{T_0}\left(\frac{\partial T}{\partial y}\right)^2\right\} \tag{4}$$

Equation of species concentration:

$$u\left(\frac{\partial C}{\partial x}\right)+v\left(\frac{\partial C}{\partial y}\right)=D_S\left(\frac{\partial^2 C}{\partial x^2}+\frac{\partial^2 C}{\partial y^2}\right)+\frac{D_T}{T_0}\left(\frac{\partial^2 T}{\partial x^2}+\frac{\partial^2 T}{\partial y^2}\right) \tag{5}$$

The boundary conditions are as follows:

$$u=L_1\left(\frac{\partial u}{\partial r}\right), v=L_1\left(\frac{\partial v}{\partial r}\right),$$

$$T=T_1+L_2\left(\frac{\partial T}{\partial r}\right), C=C_1+L_3\left(\frac{\partial C}{\partial r}\right),$$

$$\text{on}\left(x-\frac{d}{2}\right)^2+\left(y-\frac{d}{2}\right)^2=r^2$$

$$u=0, v=0, T=T_0, C=C_0 \text{ at } y=d$$
$$u=0, v=0, T=T_1, C=C_1 \text{ at } y=0 \tag{6}$$

We initiate the following non-dimensional parameters:

$$X=\frac{x}{d}, Y=\frac{y}{d}, U=\frac{ud}{\nu_f}, V=\frac{ud}{\nu_f},$$
$$\theta=\frac{T-T_0}{T_1-T_0}, S=\frac{C-C_0}{C_1-C_0} \tag{7}$$

The following are the CuO-water nanofluid properties

$$\rho_{nf}=\rho_f-\phi\rho_f+\phi\rho_s \tag{8}$$

$$(\rho C_p)_{nf}=(\rho C_p)_f-\phi(\rho C_p)_f+\phi(\rho C_p)_s \tag{9}$$

$$\frac{k_{nf}}{k_f}=\frac{(k_s+2k_f)-2\phi(k_f-k_s)}{(k_s+2k_f)+2\phi(k_f-k_s)} \tag{10}$$

Related formulas including Einstien's

$$\frac{\mu_{nf}}{\mu_f} = \frac{1}{(1-\varphi)^{0.25}} \tag{11}$$

$$(\rho\beta)_{nf} = (\rho\beta)_f - \phi(\rho\beta)_f + \phi(\rho\beta)_s, \alpha_{nf} = \frac{k_{nf}}{(\rho C_p)_{nf}} \tag{12}$$

Following are the Thermo physical properties of copper (CuO) and water

Table 1. Thermo physical values

Physical properties	Copper (CuO)	Water
c_p (J/kg/k)	385	4,179
ρ(kg/ m)	8,933	997.1
K(W/mk)	401	0.613
β_T X10^{-5} (1/K)	1.67	27.6
μ(kg m^{-1} s^{-1})	-----	8.55x10^{-4}

From the above, the equations from (1) to (5) will get the following forms

$$\frac{\partial U}{\partial X} + \frac{\partial V}{\partial Y} = 0 \tag{13}$$

$$\left.\begin{array}{c} U = \lambda\left(\frac{\partial U}{\partial R}\right), V = \lambda\left(\frac{\partial V}{\partial R}\right), \theta = 1 + \beta\left(\frac{\partial \theta}{\partial R}\right), S = 1 + \delta\left(\frac{\partial S}{\partial R}\right), \\ on\left(X - \frac{1}{2}\right)^2 + \left(Y - \frac{1}{2}\right)^2 = R^2 \\ U = 0, V = 0, \theta = 0, S = 0 at Y = '1' \\ U = 0, V = 0, \theta = 1, S = 1 at Y = '0' \end{array}\right\} \tag{14}$$

$$\left.\begin{array}{c} U\left(\frac{\partial V}{\partial X}\right) + V\left(\frac{\partial V}{\partial Y}\right) = \frac{\nu_{nf}}{\nu_f}\left(\frac{\partial^2 V}{\partial X^2} + \frac{\partial^2 V}{\partial Y^2}\right) - MV \\ -\gamma\left(U^2\frac{\partial^2 V}{\partial X^2} + V^2\frac{\partial^2 V}{\partial Y^2} + 2UV\frac{\partial^2 V}{\partial X\,\partial Y}\right) \\ +\left(1 - \phi + \phi\left(\frac{\rho_s\beta_{Ts}}{\rho_f\beta_{Tf}}\right)\right)Gr\theta + \left(1 - \phi + \phi\left(\frac{\rho_s\beta_{Cs}}{\rho_f\beta_{Cf}}\right)\right)GcS \end{array}\right\} \tag{15}$$

$$\left.\begin{array}{c} U\left(\frac{\partial \theta}{\partial X}\right) + V\left(\frac{\partial \theta}{\partial Y}\right) = \frac{1}{\Pr\left(\frac{k_{nf}}{k_f}\right)\left(\frac{(\rho C_p)_f}{(\rho C_p)_{nf}}\right)\left(\frac{\partial^2\theta}{\partial X^2} + \frac{\partial^2\theta}{\partial Y^2}\right)} \\ Nb\left(\frac{\partial S}{\partial X}\frac{\partial \theta}{\partial X} + \frac{\partial S}{\partial Y}\frac{\partial \theta}{\partial Y}\right) + Nt\left(\left(\frac{\partial \theta}{\partial X}\right)^2 + \left(\frac{\partial \theta}{\partial Y}\right)^2\right) \end{array}\right\} \tag{16}$$

$$U\left(\frac{\partial S}{\partial X}\right) + V\left(\frac{\partial S}{\partial Y}\right) = Le\left(\frac{\partial^2 S}{\partial X^2} + \frac{\partial^2 S}{\partial Y^2}\right) + \frac{Nt}{Nb}\left(\frac{\partial^2 \theta}{\partial X^2} + \frac{\partial^2 \theta}{\partial Y^2}\right) \tag{17}$$

The boundary conditions given in (6) becomes

$$\left.\begin{array}{c} U = \lambda\left(\frac{\partial U}{\partial R}\right), V = \lambda\left(\frac{\partial V}{\partial R}\right), \theta = 1 + \beta\left(\frac{\partial \theta}{\partial R}\right), S = 1 + \delta\left(\frac{\partial S}{\partial R}\right), \\ on\left(X - \frac{1}{2}\right)^2 + \left(Y - \frac{1}{2}\right)^2 = R^2 \\ U = 0, V = 0, \theta = 0, S = 0 at Y = '1' \\ U = 0, V = 0, \theta = 1, S = 1 at Y = '0' \end{array}\right\} \tag{18}$$

Where

$Gr = \frac{d^3 g\beta_T(T_1 - T_0)}{\nu_f^2}$, $Gc = \frac{d^3 g\beta_c(C_1 - C_0)}{\nu_f^2}$, $M =$
$\gamma = \frac{\nu_f k_0}{d^2}$ $Le = \frac{D_S}{\nu_f}$, $Nb = \frac{\tau D_B(C_1 - C_0)}{\nu_f}$, $Nt = \frac{\tau D_T(T_1 - T_0)}{T_0\nu_f}$,
$\lambda = \frac{L_1}{d}$, $\beta = \frac{L_2}{d}$, $\delta = \frac{L_3}{d}$, $R = \frac{r}{d}$

The total rate of heat transfer is as follows:

$$Nu_{tot} = \frac{k_{nf}}{k_f d}\int_0^d \frac{\partial \theta}{\partial X} dY,\ Sh_{tot} = Le\int_0^d \frac{\partial S}{\partial X} dY \tag{19}$$

The numerical solution for a flow, heat, and mass transfer problem is obtained using Mathematica 10.1, using the Finite Element Method (FEM). The findings are displayed through stream and contour plots, and the heat transfer rate is displayed in tables. The computational domain is splitted and it is of 969 elements, with the element count fixed based on a trial-and-error convergence test. Parameter analysis remains constant, with parameters set to ϕ = 3 %, β = Nt = λ = δ = Nb = Ln = 0.5, Gr = M = Gc = 5.Multiple slip effects were not taken into account by earlier researchers, and the channel's heating and cooling chambers might not have a major impact on the fluid's ability to transport heat effectively. Following validation by comparing results with the appropriate parameters, the model was determined to be in excellent agreement, which can be seen in Table 2.

Table 2. Comparison of results with the literature

Ra	10^3	10^4	10^5
Present Study	1.12435	2.25234	4.50531
ZoubairBoulahia et.al [27]	1.116	2.24	4.485

3.0 Result and Discussion

Stream and contour plots are self-explanatory tools used to display findings in various settings, with blue indicating a higher concentration of physical phenomena.

3.1 Stream Plots for Several Iterations of Relevant Parameters

The presented stream plots depict different CuO nanoparticle concentrations in water. Notably, for concentrations below 5 % CuO, the stream flows away from the internal heat source. A notable transition in flow pattern occurs specifically at 2 % CuO concentration. This suggests that the presence of additional internal heat sources will exert dominance over the flow pattern. The transition likely occurs due to changes in fluid

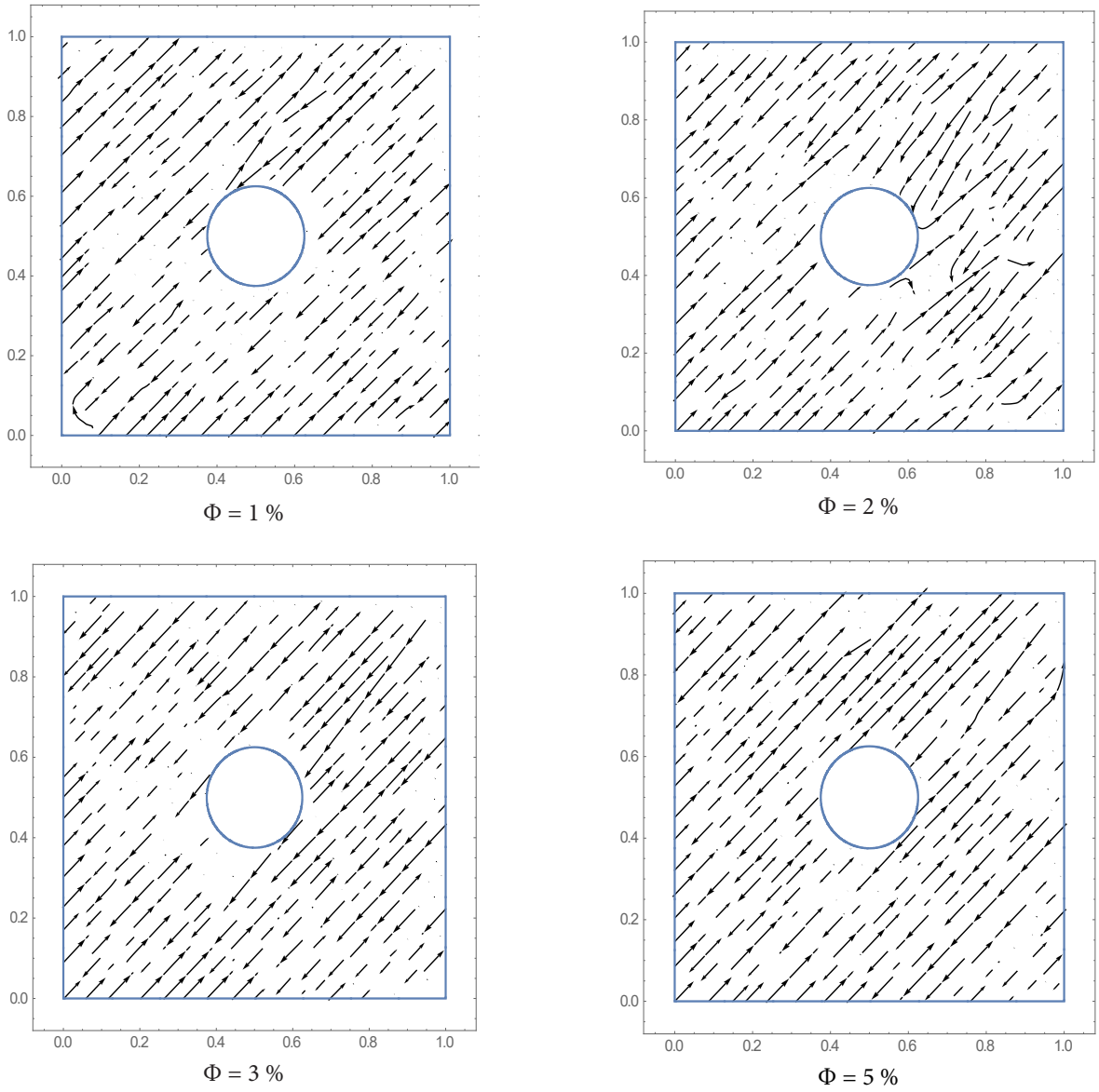


Figure 2. Stream plots for different nano particle volume fractions.

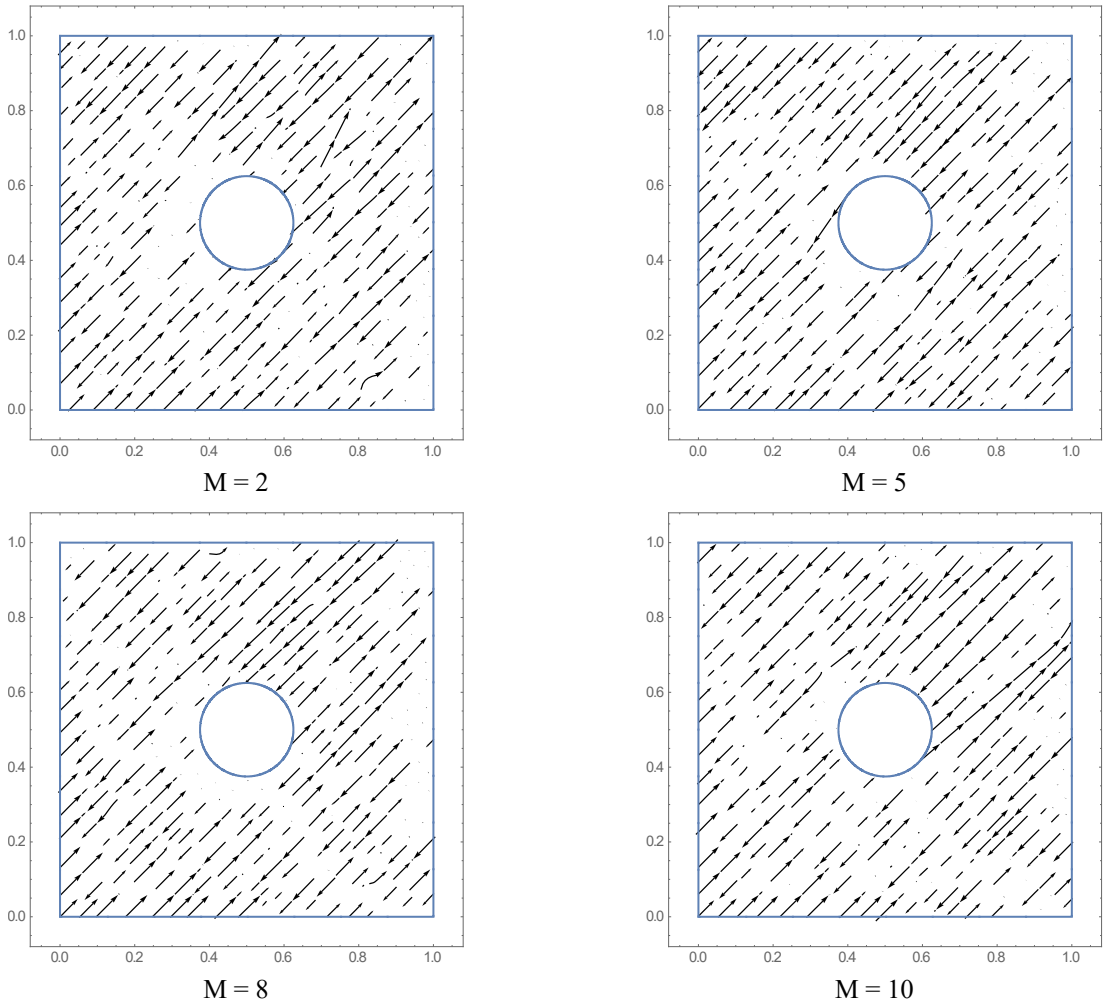
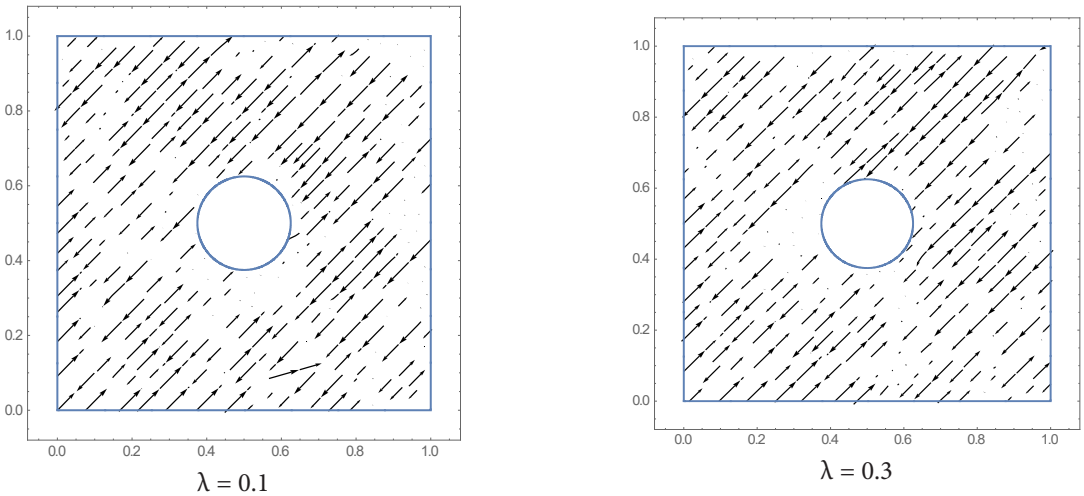


Figure 3. Stream graphs for various magnetic parameter values.



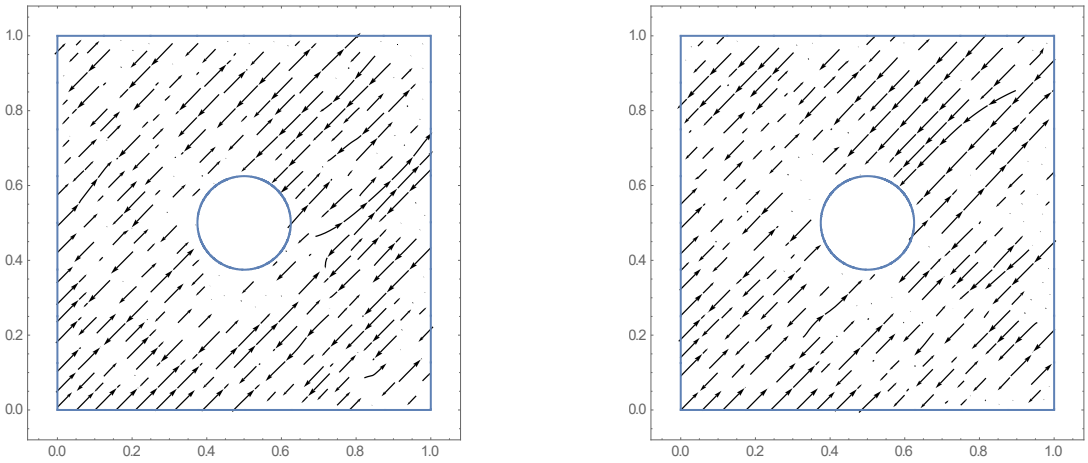


Figure 4. Stream plots: velocity slip parameter.

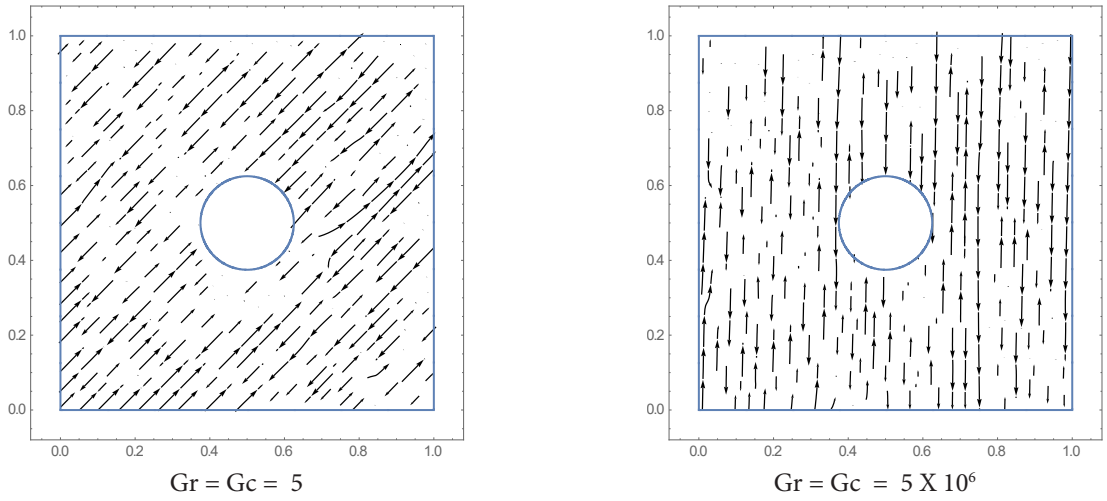


Figure 5. Stream plots : thermal and molecular grashoff numbers.

properties and interactions between nanoparticles and the flow field, highlighting the sensitivity of flow patterns to nanoparticle concentrations. Understanding these variations is crucial for predicting and controlling heat transfer in nanoparticle-enhanced fluids.

The presented stream plots illustrate varying magnetic parameter values, demonstrating the influence of controlled magnetic fields on flow regulation. Notably, at lower magnetic field strengths, the flow pattern tends towards irregularity. This highlights the critical role of magnetic fields in governing flow behavior, as they exert control over fluid motion. The irregularity observed at lesser magnetic field strengths is likely due to weaker magnetic forces, allowing for more chaotic flow patterns.

The slip parameter represents the ability of fluid molecules to slip past a solid boundary, influencing the fluid flow near the boundary. At moderate velocities around 0.3, the slip effect becomes noticeable, causing a reduction in flow intensity around the heat source. This reduction occurs because slip allows fluid molecules to move more freely near the boundary, resulting in less resistance to flow. In convective heat and mass transfer processes, this altered flow dynamics affect the transfer rates of heat and mass.

The observed stream pattern indicates a pronounced influence of buoyancy on the flow field dynamics. As Grashoff numbers increase, there's a notable alteration in the flow direction. However, at higher Grashoff

numbers, the effectiveness of velocity slip diminishes. This implies that although buoyancy-driven forces continue to be important in determining flow patterns, velocity slip's influence diminishes as Grashoff numbers rise. Consequently, at elevated Grashoff numbers, other factors such as thermal gradients may dominate flow behavior, rendering velocity slip less effective in altering flow dynamics.

3.2 Contour Plots for Different Variations of Pertinent Parameters

The temperature contours depict CuO nanoparticle

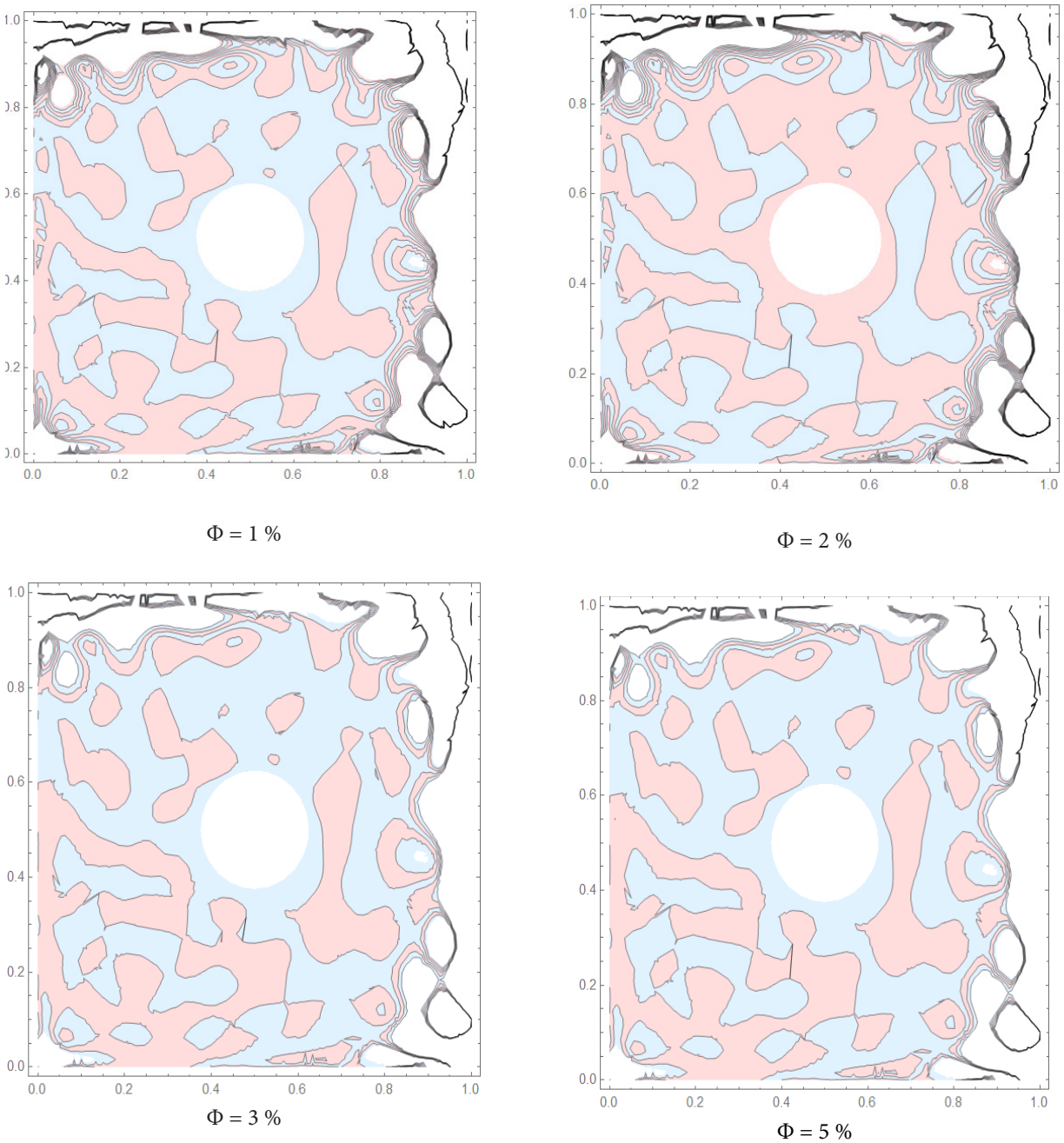


Figure 6. The temperature contours: nanoparticle volume fractions.

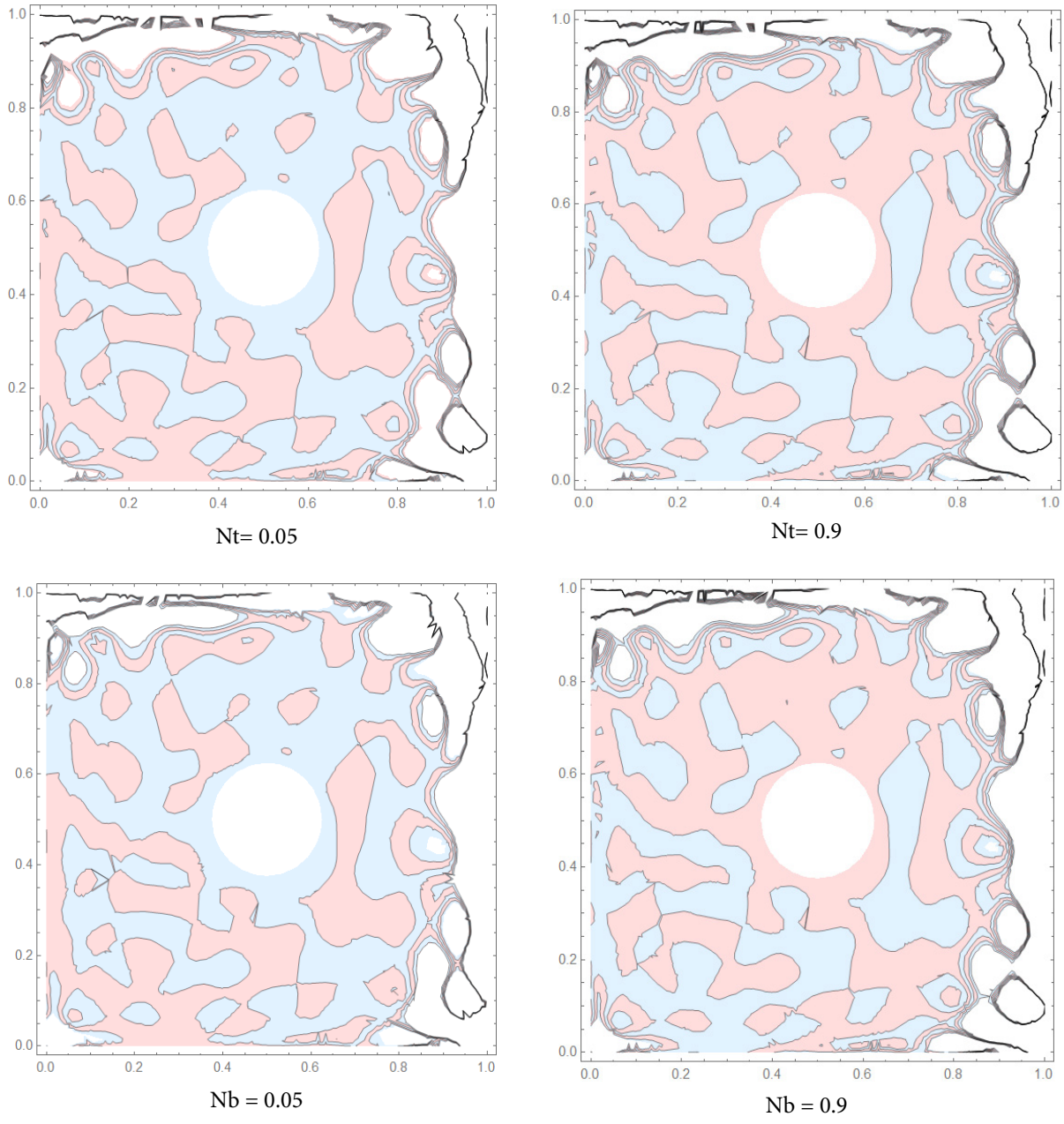


Figure 7. The temperature contours for different values of thermophoresys and Brownian parameters.

concentrations in water, with blue indicating higher temperatures. Higher CuO volume fractions correlate with elevated temperatures in the region. Notably, around 2 % CuO particles in water, the internal heat source exhibits diminished effectiveness. This observation suggests that certain concentrations of CuO nanoparticles may alter heat transfer dynamics, possibly due to changes in fluid properties or thermal conductivity

Thermophoresis and Brownian motion parameters demonstrate analogous effects on temperature distribution throughout the region. Around 0.9 for both parameters, the influence of the internal heat source is

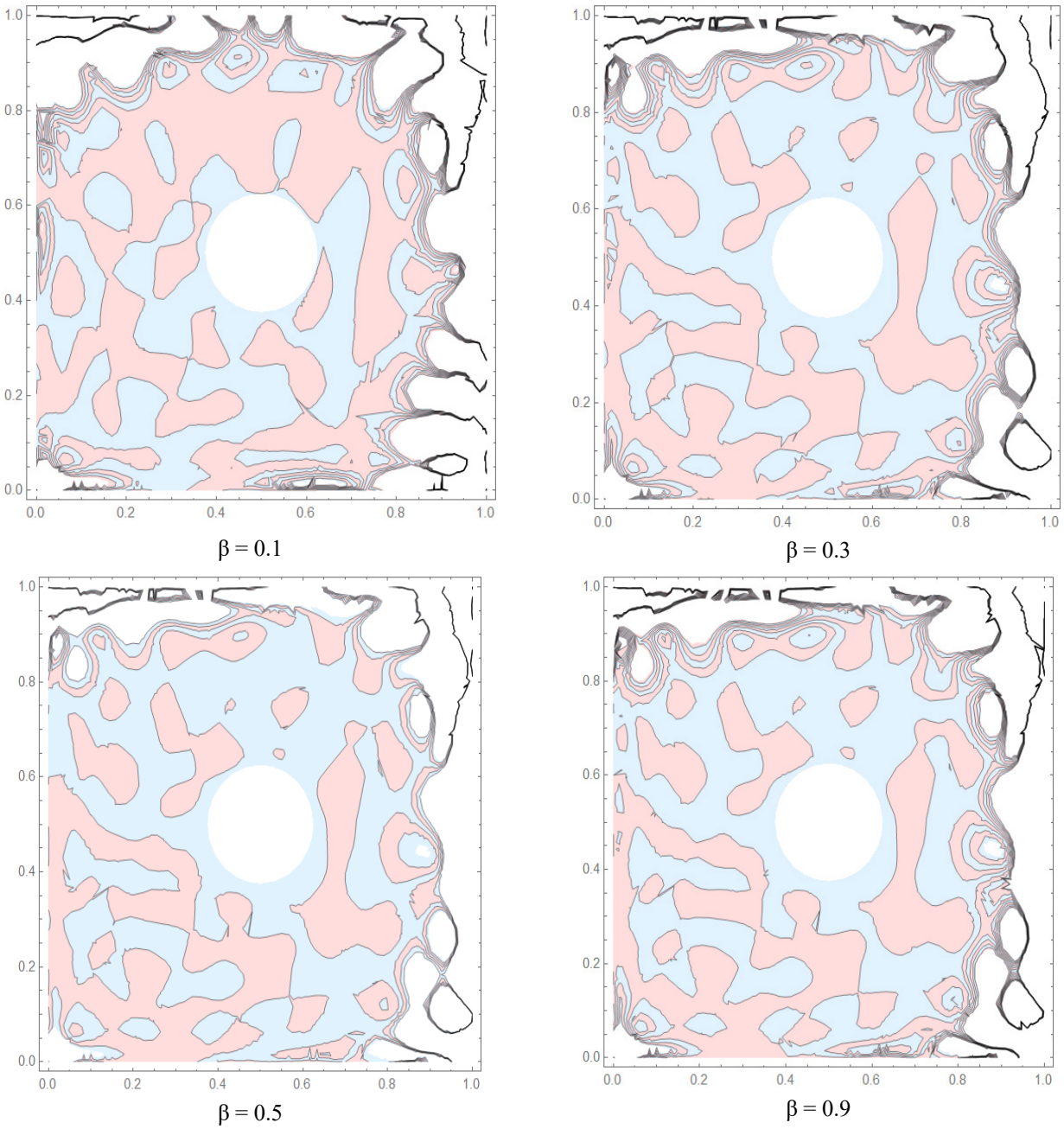


Figure 8. The temperature contours: thermal slip parameters.

notably subdued. This suggests that, at this value, CuO particle movement prevails, even in the presence of both external and internal heat sources. Such behavior underscores the dominance of CuO particle dynamics in shaping temperature profiles, potentially overshadowing the thermal effects of external and internal heat sources.

The observed phenomenon concerns the thermal slip effects on temperature distribution. Higher thermal slip at the internal heat source leads to an augmentation of temperature in the region. Notably, the temperature dispersion is evident from both external and internal heat sources. This suggests that thermal slip plays a significant

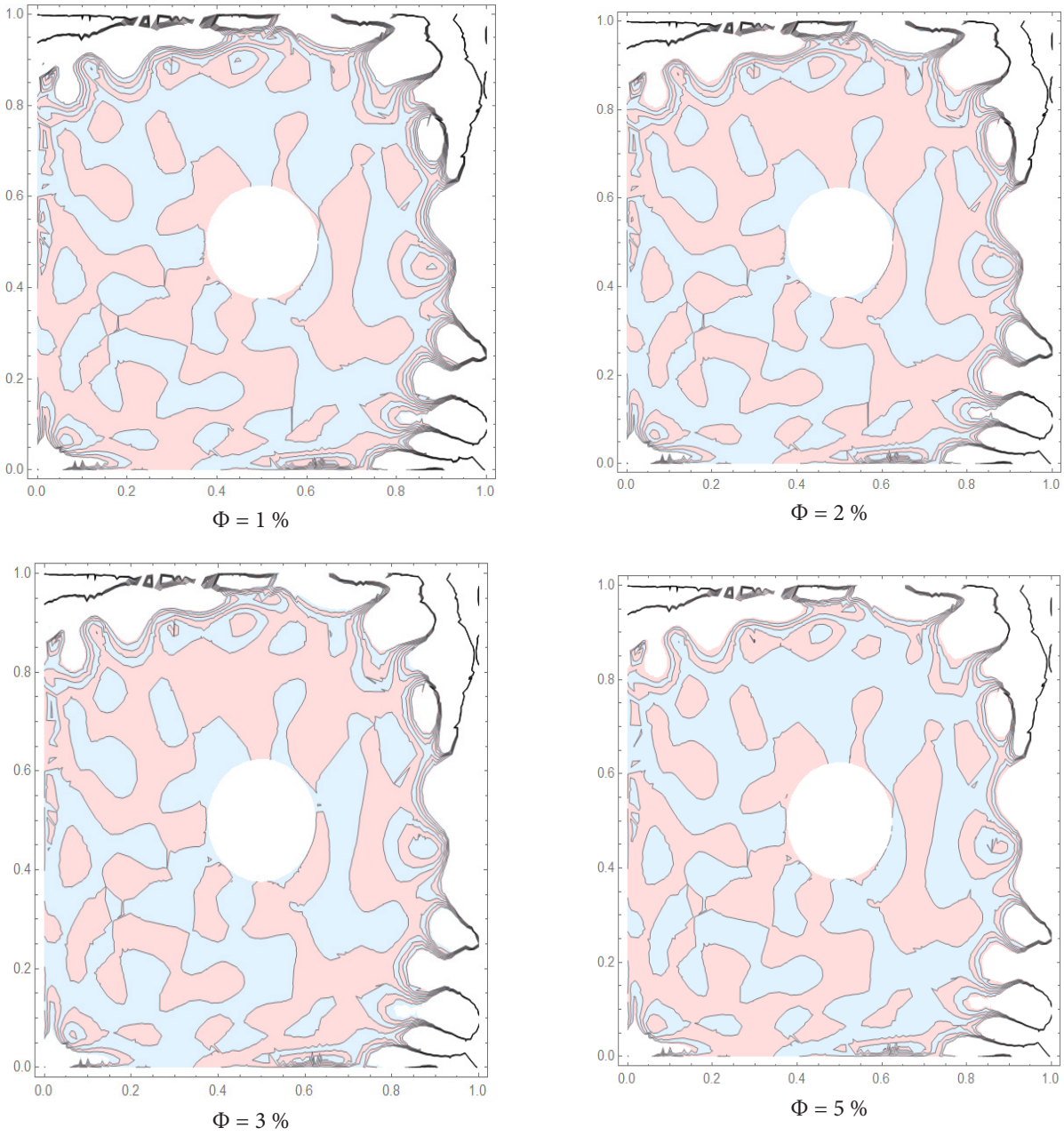


Figure 9. The diffusion contours: nanoparticle volume fractions.

role in modulating temperature profiles, particularly around heat sources.

Increased diffusion rates are correlated with 5% CuO nanoparticles in water, demonstrating the strong influence of Brownian motion.This increased diffusion is likely due to the enhanced movement of nanoparticles within the fluid, driven by Brownian motion.

The study reveals that flow dynamics are primarily influenced by a small amount of diffusion slip, with higher levels facilitating efficient flow distribution.

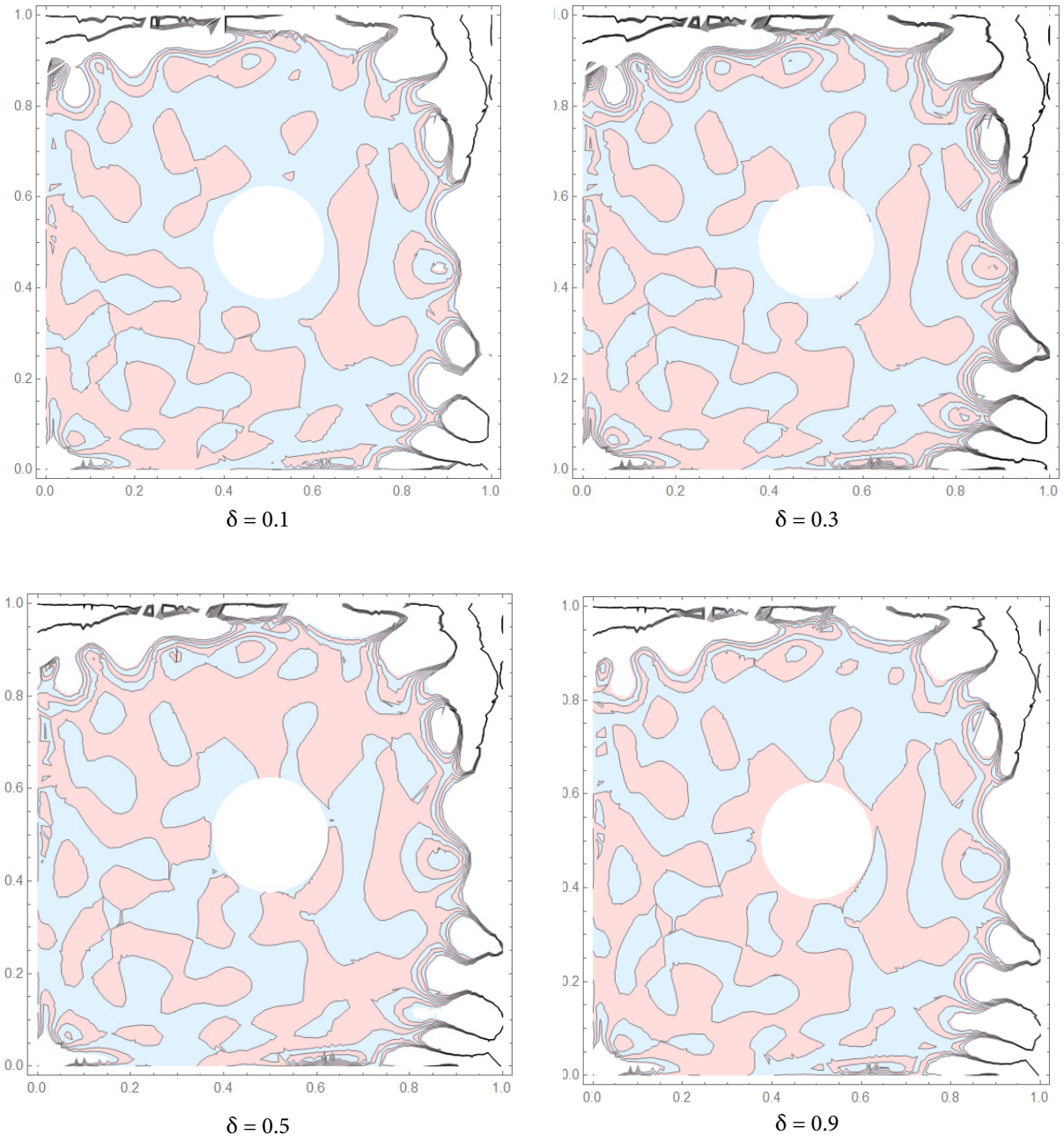


Figure 8. The diffusion contours: diffusion slip parameters.

3.3 Nusselt Number Values

The heat transfer rate and mass transfer rate are calculated for variations of φ, β, Nb, Nt. The results are displayed in the following table.

The increase in metal particle proportion from 1 % to 5 % clearly shows the increase in heat transfer rate from the source to the fluid. The Brownian motion also increases slightly. But on the other hand thermophorosys parameter enhances the heat transfer rate notably,

Table 3. Nusselt nuber and Sherwood numbers for different parameters

φ	Nu	Sh		Nb	Nu	Sh		Nt	Nu	Sh
1 %	1.63424	1.37565		0.3	1.77505	2.05973		0.3	1.65188	0.44329
2 %	1.71267	1.22838		0.5	1.79221	1.09748		0.5	1.79221	1.09748
3 %	1.79221	1.09748		0.9	1.79978	0.501058		0.9	2.09402	4.19065
5 %	1.95007	0.86481		1	1.80217	0.444276		1	2.18446	5.63073
β	Nu			δ	Sh					
0.1	21.421			0.1	0.696799					
0.3	2.76471			0.3	0.964783					
0.5	1.79221			0.5	1.09748					

pronouncing the presence of additional heat source. Interestingly the increase in thermal slip reduces the heat transfer rate rapidly. Therefore, according to industrial needs, it is more beneficial to include thermal slip into heating or cooling systems.

4.0 Conclusion

This study introduces a unique investigation of heat and mass transfer within a Maxwell nanofluid through a horizontal channel with a centrally heated cylindrical geometry, examining slip effects on flow control, with potential applications in industrial heat and mass transfer processes.

The findings open avenues for customized nanofluid systems in industries where precise heat and mass transfer control is essential, such as in microelectronics cooling and chemical reactors.

The results highlight the necessity of carefully evaluating nanoparticle concentrations in order to improve heat transfer mechanisms. Optimizing heat transfer performance in real-world applications requires more research and comprehension of these processes.

All things considered, these results highlight the intricate interactions between buoyancy forces, slip parameters, and magnetic fields that shape flow patterns.

5 % CuO nanoparticles in water correlates with heightened diffusion rates, attributed to the pronounced effect of Brownian motion. This increased diffusion underscores the influence of nanoparticle movement driven by Brownian motion.

There is a notable enhancement in the heat transfer rate, indicating the effectiveness of higher metal particle concentrations in facilitating heat transfer processes.

The thermophoresis parameter notably enhances the heat transfer rate, underscoring the influence of additional heat sources in augmenting heat transfer processes.

The substantial effect of thermal slip on heat transfer rates is also shown in the study.

The findings underscore the importance of metal particle concentration, Brownian motion, thermophoresis, and thermal slip in influencing heat transfer rates. Understanding these factors can aid in optimizing heat transfer processes in various industrial applications.

Nusselt number rises with increasing nanoparticle concentration (ϕ\phiϕ), showing enhanced heat transfer, but decreases with higher thermal slip (β). This indicates

that nanoparticle concentration and thermal slip can be strategically tuned to control heat transfer efficiency.

The increase in Sherwood number with higher diffusion slip (δ) suggests that diffusion slip effectively enhances mass transfer, while higher nanoparticle concentrations reduce Sh. This implies that carefully adjusting these parameters can optimize solute transport.

Future studies should explore a broader range of slip parameters, nanoparticle types, and geometries to enhance heat and mass transfer efficiency across diverse engineering applications.

5. References

1. Gul T, Nasir S, Berrouk AS, Raizah Z, Alghamdi W, Ali I, *et al*. Simulation of the water-based hybrid nanofluids flow through a porous cavity for the applications of the heat transfer. Sci Rep. 2023; 13(1):7009. https://doi.org/10.1038/s41598-023-33650-w
2. Rashid FL, Al-Gaheeshi AMR, Alhwayzee M, Ali B, Shah NA, Chung JD. Mixed convection in a horizontal channel-cavity arrangement with different heat source locations. Mathematics. 2023; 11:1428. https://doi.org/10.3390/math11061428
3. Vanaja G, Srinivas G, Babu BS, Goud BS, Hendy AS, Ali MR, *et al*. Influence of variable viscosity and slip on heat and mass transfer of immiscible fluids in a vertical channel. Case Stud Therm Eng. 2024; 104368. https://doi.org/10.1016/j.csite.2024.104368
4. Cheruku V, Reddy BR. Numerical study on the effect of thermal slip on two-fluid flow in a vertical channel. Trans Energy Syst Eng Appl. 2023; 4(2):1-18. https://doi.org/10.32397/tesea.vol4.n2.517
5. Mebarek-Oudina F, Laouira H, Aissa A, Hussein AK, El Ganaoui M. Convection heat transfer analysis in a channel with an open trapezoidal cavity: heat source locations effect. MATEC Web Conf. 2020; 330:01006. https://doi.org/10.1051/matecconf/202033001006
6. Everts M, Mahdavi M, Meyer JP, Sharifpur M. Development of the hydrodynamic and thermal boundary layers of mixed convective laminar flow through a horizontal tube with a constant heat flux. Int J Therm Sci. 2023; 187:108178. https://doi.org/10.1016/j.ijthermalsci.2022.108098
7. Ali MM, Akhter R, Miah MM. Hydromagnetic mixed convective flow in a horizontal channel equipped with Cu-water nanofluid and alternated baffles. Int J Thermofluids. 2021; 12:100118. https://doi.org/10.1016/j.ijft.2021.100118
8. Mashkour MA. Analysis of transient mixed convection in a horizontal channel partially heated from below. East Eur J Enterp Technol. 2021; 4(8):16-22. https://doi.org/10.15587/1729-4061.2021.238649
9. Alguboori AR, Al-Azzawi MM, Kalash AR, Habeeb LJ. Natural convection heat transfer in an inclined elliptic enclosure with circular heat source. J Mech Eng Res Dev. 2020; 43(6):207-222.
10. Noor NA, Shafie S, Admon MA. Slip effects on MHD squeezing flow of Jeffrey nanofluid in a horizontal channel with chemical reaction. Mathematics. 2021; 9(11):1215. https://doi.org/10.3390/math9111215
11. Zohra FT, Uddin MJ, Ismail A. Magnetohydrodynamic bio-nanoconvective Naiver slip flow of micropolar fluid in a stretchable horizontal channel. Heat Transf-Asian Res. 2019; 48(8):3636-3656. https://doi.org/10.1002/htj.21560
12. Gorbachev M, Terekhov V. Simulating heat and mass transfer processes during water film evaporation in a horizontal channel. J Phys Conf Ser. 2020; 1675(1). https://doi.org/10.1088/1742-6596/1675/1/012057
13. Nazeer M, Irfan M, Hussain F, Siddique I. Entropy generation analysis in blood-gold Casson nanofluid through horizontal wavy channel with velocity and thermal slips: applications in skin diseases. J Comput Biophys Chem. 2023; 22(3):259-272. https://doi.org/10.1142/S2737416523400021
14. Felicita A. Slip and convective flow of Williamson nanofluid influenced by Brownian motion and thermophoresis mechanism in a horizontal microchannel. Proc Inst Mech Eng Part N J Nanomater Nanoeng Nanosyst. 2023; 23977914231177340. https://doi.org/10.1177/23977914231177340
15. Babu DH, Reddy SH, Naidu KK, Narayana PVS, Venkateswarlu B. Numerical investigation for entropy-based magneto nanofluid flow over non-linear stretching surface with slip and convective boundary conditions. ZAMM J Appl Math Mech. 2023. https://doi.org/10.1002/zamm.202300006
16. Mahmood Z, Eldin MS, Rafique K, Khan U. Numerical analysis of MHD tri-hybrid nanofluid over a nonlinear stretching/shrinking sheet with heat generation/absorption and slip conditions. Alex Eng J. 2023; 76:799-819. https://doi.org/10.1016/j.aej.2023.06.081
17. Boujelbene M, Rehman S, Jazaa Y, Dhaou MH. Thermodynamics of hydromagnetic boundary layer

flow of Prandtl nanofluid past a heated stretching cylindrical surface with interface slip. J Taiwan Inst Chem Eng. 2024; 155:105310. https://doi.org/10.1016/j.jtice.2023.105310

18. Adnan MA, Mudassar R. The effect of Nusselt number on the bi-viscosity fluid subjected to the discrete heating effect. J Therm Eng. 2021; 7(7):1797-1814. http://dx.doi.org/10.18186/thermal.1026010
19. Cheruku V, Reddy BR. Numerical analysis of heat and mass transfer in a vertical channel with multiple slip effect. Int J Interact Des Manuf. 2023; 1-11. https://doi.org/10.32397/tesea.vol4.n2.517
20. Srikanth GVP, Srinivas G, Suresh Babu B, Srilatha R. Heat and mass transfer flow of nano-fluid over a stretching sheet with chemical reactions. AIP Conf Proc. 2020;2246(1). https://doi.org/10.1063/5.0017783
21. Sailaja B, Srinivas G, Suresh Babu B. Free and forced convective heat transfer through a nanofluid in two dimensions past a moving vertical plate. South East Asian J Math Math Sci. 2020; 16. https://doi.org/10.36963/IJTST.2020070302
22. Lone SA, Raizah Z, Saeed A, Bognár G. Statistical computation for heat and mass transfers of water-based nanofluids containing Cu, Al_2O_3, and TiO_2 nanoparticles over a curved surface. Sci Rep. 2024; 14(1):6908. http://dx.doi.org/10.1038/s41598-024-57532-x
23. Gosty V, Srinivas G, Suresh Babu B. Numerical investigation of slip effects on heat and mass transfer in a vertical channel with immiscible micropolar and viscous fluids of variable viscosity. Heat Transf. 2024. http://dx.doi.org/10.1002/htj.23120
24. Khan SA, Imran M, Waqas H, Muhammad T, Yasmin S, Alhushaybari A. Numerical analysis of multiple slip effects on CuO/MgO/TiO_2-water ternary hybrid nanofluid with thermal and exponential space-based heat source. Tribol Int. 2024; 197:109778. http://dx.doi.org/10.1016/j.triboint.2024.109778
25. Khan ZH, Khan WA, Ibrahim SM, Swain K, Huang Z. Impact of multiple slips and thermal radiation on heat and mass transfer in MHD Maxwell hybrid nanofluid flow over a porous stretching sheet. Case Stud Therm Eng. 2024; 61:104906. https://doi.org/10.1016/j.csite.2024.104906
26. Kumar A, Yadav PK. An inclined magnetic field and slip effect on heat and mass transfer analysis in the peristaltic flow of immiscible fluid through an asymmetric porous channel. Int Commun Heat Mass Transf. 2024; 159(B):108118. https://doi.org/10.1016/j.icheatmasstransfer.2024.108118
27. Boulahia Z, Wakif A, Chamkha AJ, Sehaqui R. Numerical study of natural and mixed convection in a square cavity filled by a Cu-water nanofluid with circular heating and cooling cylinders. Mech Ind. 2017; 18:502. https://doi.org/10.1051/meca/2017044
28. Babu NVN, Gundagani M, Paul A. Soret and Dufour effects on unsteady hydromagnetic free convective fluid flow past an infinite vertical porous plate in the presence of chemical reaction. J Sci Arts. 2015; 15(1):99-111.
29. Babu NVN, Murali G, Bhati SM. Casson fluid performance on natural convective dissipative Couette flow past an infinite vertically inclined plate filled in a porous medium with heat transfer, MHD, and Hall current effects. Int J Pharm Res. 2018; 10(4):809-819.
30. Gundagani M, Babu, NVN. Effect of Radiation on MHD Convection Flow Past a Vertical Permeable Moving Plate. Int J Advances in Appl; (IJAAS)2012; 1(1):19-28
31. Deepa G, Murali G. Effects of viscous dissipation on unsteady MHD free convective flow with thermophoresis past a radiate inclined permeable plate. Iran J Sci Technol Sci. 2014; 38A(3). https://doi.org/10.22099/IJSTS.2014.2437
32. Deepa G, Gundagani M. Analysis of Soret and Dufour effects on unsteady MHD flow past a semi-infinite vertical porous plate via the finite difference method. Int J Appl Phys Math. 2014; 4(5):332-344. https://doi.org/10.7763/IJAPM.2014.V4.306
33. Gundagani M, Babu NVN, Gadially D, Bhati SM, Sanjay Ch, Nirmala Kasturi V. Study of Nano-Powell-Erying fluid flow past a porous stretching sheet by the effects of MHD, thermal and mass convective boundary conditions. J Umm Al-Qura Univ Eng Archit. 2024; 15:271-281. https://doi.org/10.1007/s43995-024-00056-2
34. Kirubaharan DR, Subhashini AD, Murali G. Study of three dimensional casson-nanofluid flow due to a linear porous stretching sheet in the presence of double diffusion effects. Advances in Systems Science and Applications. 2024; 24(3): 90-103. https://doi.org/10.25728/assa.2024.2024.03.1539
35. Sivaiah S, Gundagani M, Karanamu MP. Analysis of heat and mass transfer effects on an isothermal vertical oscillating plate. Walailak J Sci Tech. (WJST). 2012;

9(4):407–415. https://wjst.wu.ac.th/index.php/wjst/article/view/451
36. Murali G, Deepa G, Venkata Madhu J, Nirmala Kasturi V, Bhati SM, Narendra Babu N. Three dimensional chemically reacting oldroyd-B fluid + nanofluid flow in presence of thermophoresis and brownian motion effects, discontinuity, nonlinearity, and complexity. 2025; 14(2):373-388. https://doi. org/10.5890/DNC.2025.06.010
37. Gundagani M, Mamidi LP, Tanuku PK. Finite element solutions of double diffusion effects on three-dimensional MHD Nano-Powell-Erying fluid flow in presence of thermal and mass Biot numbers. J Eng Appl Sci. 2024b; 71. https://doi.org/10.1186/ s44147-023-00347-w
38. Gundagani M, Sheri S, Paul A, Reddy MCK. Unsteady magnetohydrodynamic free convective flow past a vertical porous plate. Int J Appl Sci Eng. 2013; 11(3):267-275.
39. Murali G, Paul A, Babu NVN. Heat and mass transfer effects on an unsteady hydromagnetic free convective flow over an infinite vertical plate embedded in a porous medium with heat absorption. Int J Open Probl Comput Math. 2015; 8(1):15-27. https://doi.org/10.12816/0010706
40. Tanuku PK, Mamidi LP, Gundagani M. Modelling and analysis of three-dimensional chemically reacting, radiating Casson-nanofluid flow: thermophoresis and Brownian motion effects. Acta Polytech. 2024; 64(5):455-463. https://doi.org/10.14311/AP.2024.64.0455
41. Bhati SM, Murali G, Sanjay C. Law of electric fields via Bianchi identities. J Appl Sci Eng. 2022; 25(4). https://doi.org/10.6180/jase.202208_25(4).0011
42. Murali G, Paul A, Babu NVN. Numerical study of chemical reaction effects on unsteady MHD fluid flow past an infinite vertical plate embedded in a porous medium with variable suction. Electron J Math Anal Appl. 2015; 3(2):179-192. https://doi.org/10.21608/ejmaa.2015.310762
43. Murali G, Deepa G, Kasturi VN, Poornakantha T. Joint effects of thermal diffusion and diffusion thermo on MHD three-dimensional nanofluid flow towards a stretching sheet. Math Models Eng. 2023. https://doi.org/10.21595/mme.2023.23590
44. Murali G, Babu NVN. Convective MHD Jeffrey fluid flow due to vertical plates with pulsed fluid suction: A numerical study. J Comput Appl Mech. 2023; 54(1):36-48. https://doi.org/10.22059/JCAMECH.2023.351326.773
45. Murali G, Reddy MCK, Sivaiah. Finite element solution of thermal radiation effect on unsteady MHD flow past a vertical porous plate with variable suction. American Academic and Scholarly Research Journal. 2012; 4(3):3-22.
46. Gundagani M, Sheri S, Reddy MCK. Soret and Dufour effects on unsteady MHD mixed convection flow past a vertical porous plate with thermal radiation. Caspian J Appl Sci Res. 2012; 1(9). https://doi.org/10.14419/ijbas.v1i4.106
47. Reddy MK, Murali G, Sivaiah S, Babu NVN. Heat and mass transfer effects on unsteady MHD free convection flow past a vertical permeable moving plate with radiation. Int J Appl Math Res. 2012; 1(2):189-205. https://doi.org/10.14419/ijamr.v1i2.45
48. Singh N, Kaur J, Thakur P, Gundagani M. Structural behaviour of annular isotropic disk made of steel/copper material with gradually varying thickness subjected to internal pressure. Struct Integr Life. 2023; 23(3):293-297
49. Sivaiah S, Gundagani M, Karanamu MP. Analysis of heat and mass transfer effects on an isothermal vertical oscillating plate. Walailak J Sci Tech. 2012; 9(4):407-415. https://doi.org/10.5402/2012/401515
50. Sivaiah S, Muraligoud G, Murali G, Reddy MCK. Unsteady MHD mixed convection flow past a vertical porous plate in presence of radiation. Int J Basic Appl Sci. 2012; 1(4):651-666. https://doi.org/10.14419/ijbas.v1i4.106
51. Tanuku P, Mamidi L, Gundagani M. Modelling and analysis of three-dimensional Maxwell-Nanofluid Flow over a bi-directional stretching surface in the presence of a magnetic field. Int J Eng Model. 2025; 38(1):53-72. https://doi.org/10.31534/engmod.2025.1.ri.04d
52. Nagasmitha BR, Nagendramma V, Ahmed N, Marutamanikandan S, Murali G. Analytical study of nonlinear behavior and convection patterns in darcy-brinkman porous medium with Maxwell-Cattaneo ferroconvection. Journal of Mines, Metals and Fuels. 2025; 73(2):437–445. https://doi.org/10.18311/jmmf/2025/47828
53. Nagasmitha BR, Nagendramma V, Ahmed N, Marutamanikandan S, Murali G. Mathematical modeling of heat transfer phenomena in darcy porous media with couple-stress magnetic fluid under Maxwell-Cattaneo model. Journal of Mines, Metals and

Fuels. 2025; 73(2):509–516. https://doi. org/10.18311/jmmf/2025/47825

54. Mebarek-Oudina F, Dharmaiah G, Balamurugan KS, Ismail AI, Saxena H. The role of quadratic- linearly radiating heat source with carreau nanofluid and exponential space-dependent past a cone and a wedge: A medical engineering application and renewable energy. Journal of Computational Biophysics and Chemistry. 2023; 22(8):997-1011. https://doi.org/10.1142/S2737416523420073
55. Dharmaiah G, Mebarek-Oudina F, Rama Prasad JL, Ch. Rani B. Exploration of bio-convection for slippery two-phase Maxwell Nanofluid past a vertical induced magnetic stretching regime associated for biotechnology and engineering. Journal of Molecular Liquids. 2023; 391:123408. https://doi.org/10.1016/j.molliq.2023.123408
56. Ramesh K, Mebarek-Oudina F, Souayeh B. Mathematical Modelling of Fluid Dynamics and Nanofluids, 1st ed. CRC Press (Taylor & Francis); 2023. https://doi.org/10.1201/9781003299608
57. Raza J, Mebarek-Oudina F, Ali H, Sarris IE. Slip effects on Casson Nanofluid over a Stretching sheet with activation energy: RSM Analysis, Frontiers in Heat and Mass Transfer. 2024; 22(4):1017-1041. https://doi.org/10.32604/fhmt.2024.052749
58. Ould Said B, Mebarek-Oudina F, Medebber AM. Magneto-hydro-convective nanofluid flow in porous square enclosure, Frontiers in Heat and Mass Transfer. 2024; 22(5):1343-360. https://doi.org/10.32604/fhmt.2024.054164
59. Mezaache A, Mebarek-Oudina F, Vaidya H, Ramesh K. Impact of nanofluids and porous structures on the thermal efficiency of wavy channel heat exchanger. International Journal of Thermal Sciences. 2024; 210(2025):109673. https://doi.org/10.1016/j.ijthermalsci.2024.109673